Exploring the basis for specificity in Rac function is an important task for the future. □

Methods

Mosaic analysis

Eye-specific mosaics for chromosome arm 3L were generated using *eyFLP* and *FRT80B* as described[20], using *M(3)RpS17*[4] to enhance clone size. For wing and eye clones generated using *hsFLP*, heat shocks of 1 h at 38 °C were administered at 24–48 h and again at 48–72 h of development. For germline clones, *hsFLP* was used together with an ovo^{D1} insertion[27] on the *FRT80B* chromosome (gift of K. Basler). Heterozygous third instar larvae were heat shocked for 35 min at 39 °C, and adult females crossed to males carrying the appropriate third chromosome over a TM3, *Ubx-lacZ* balancer. In order to generate germline clones in a Mtl^{Δ} homozygous background, Mtl^{Δ} was first recombined onto the ovo^{D1} *FRT80B* chromosome by FLP-induced germline recombination in males.

Histology

Embryos were fixed and stained with monoclonal antibodies 1D4, 22C10, or FMM5, as described[28]. Embryonic cuticle preparations and F-actin staining were performed as described[5], using rhodamine-conjugated phalloidin (Molecular Probes, 4 U ml^{-1}). Pupal wings and eyes were prepared and stained with rhodamine-phalloidin and mouse anti-β-galactosidase (Promega, 1:200), as described[29,30]. Adult head sections were prepared and stained as described[20].

Received 1 August 2001; accepted 31 January 2002.

1. Hall, A. Rho GTPases and the actin cytoskeleton. *Science* **279,** 509–514 (1998).
2. Luo, L. Rho GTPases in neuronal morphogenesis. *Nature Rev. Neurosci.* **1,** 173–180 (2000).
3. Eaton, S., Wepf, R. & Simons, K. Roles for Rac1 and Cdc42 in planar polarization and hair outgrowth in the wing of *Drosophila*. *J. Cell Biol.* **135,** 1277–1289 (1996).
4. Fanto, M., Weber, U., Strutt, D. I. & Mlodzik, M. Nuclear signaling by Rac and Rho GTPases is required in the establishment of epithelial planar polarity in the *Drosophila* eye. *Curr. Biol.* **10,** 979–988 (2000).
5. Harden, N., Loh, H. Y., Chia, W. & Lim, L. A dominant inhibitory version of the small GTP-binding protein Rac disrupts cytoskeletal structures and inhibits developmental cell shape changes in *Drosophila*. *Development* **121,** 903–914 (1995).
6. Luo, L., Liao, Y. J., Jan, L. Y. & Jan, Y. N. Distinct morphogenetic functions of similar small GTPases: *Drosophila* Drac1 is involved in axonal outgrowth and myoblast fusion. *Genes Dev.* **8,** 1787–1802 (1994).
7. Kaufmann, N., Wills, Z. P. & Van Vactor, D. *Drosophila* Rac1 controls motor axon guidance. *Development* **125,** 453–461 (1998).
8. Hariharan, I. K. *et al.* Characterization of Rho GTPase family homologues in *Drosophila melanogaster*: overexpressing Rho1 in retinal cells causes a late developmental defect. *EMBO J.* **14,** 292–302 (1995).
9. Adams, M. D. *et al.* The genome sequence of *Drosophila melanogaster*. *Science* **287,** 2185–2195 (2000).
10. Newsome, T. P. *et al.* Trio combines with Dock to regulate Pak activity during photoreceptor axon pathfinding in *Drosophila*. *Cell* **101,** 283–294 (2000).
11. Ng, J. *et al.* Rac GTPases control axon growth, guidance and branching. *Nature* **416,** 442–447 (2002).
12. Williams-Masson, E. M., Malik, A. N. & Hardin, J. An actin-mediated two-step mechanism is required for ventral enclosure of the *C. elegans* hypodermis. *Development* **124,** 2889–2901 (1997).
13. Jacinto, A., Martinez-Arias, A. & Martin, P. Mechanisms of epithelial fusion and repair. *Nature Cell Biol.* **3,** E117–E123 (2001).
14. Young, P. E., Richman, A. M., Ketchum, A. S. & Kiehart, D. P. Morphogenesis in *Drosophila* requires nonmuscle myosin heavy chain function. *Genes Dev.* **7,** 29–41 (1993).
15. Edwards, K. A., Demsky, M., Montague, R. A., Weymouth, N. & Kiehart, D. P. GFP-moesin illuminates actin cytoskeleton dynamics in living tissue and demonstrates cell shape changes during morphogenesis in *Drosophila*. *Dev. Biol.* **191,** 103–117 (1997).
16. Jacinto, A. *et al.* Dynamic actin-based epithelial adhesion and cell matching during *Drosophila* dorsal closure. *Curr. Biol.* **10,** 1420–1426 (2000).
17. Wakelam, M. J. The fusion of myoblasts. *Biochem. J.* **228,** 1–12 (1985).
18. Doberstein, S. K., Fetter, R. D., Mehta, A. Y. & Goodman, C. S. Genetic analysis of myoblast fusion: blown fuse is required for progression beyond the prefusion complex. *J. Cell Biol.* **136,** 1249–1261 (1997).
19. Shulman, J. M., Perrimon, N. & Axelrod, J. D. Frizzled signaling and the developmental control of cell polarity. *Trends Genet.* **14,** 452–458 (1998).
20. Newsome, T. P., Asling, B. & Dickson, B. J. Analysis of *Drosophila* photoreceptor axon guidance in eye-specific mosaics. *Development* **127,** 851–860 (2000).
21. Awasaki, T. *et al.* The *Drosophila* trio plays an essential role in patterning of axons by regulating their directional extension. *Neuron* **26,** 119–131 (2000).
22. Bateman, J., Shu, H. & Van Vactor, D. The guanine nucleotide exchange factor trio mediates axonal development in the *Drosophila* embryo. *Neuron* **26,** 93–106 (2000).
23. Liebl, E. C. *et al.* Dosage-sensitive, reciprocal genetic interactions between the Abl tyrosine kinase and the putative GEF trio reveal trio's role in axon pathfinding. *Neuron* **26,** 107–118 (2000).
24. Sone, M. *et al.* Still life, a protein in synaptic terminals of *Drosophila* homologous to GDP-GTP exchangers. *Science* **275,** 543–547 (1997).
25. Reddien, P. W. & Horvitz, H. R. CED-2/CrkII and CED-10/Rac control phagocytosis and cell migration in *Caenorhabditis elegans*. *Naure Cell Biol.* **2,** 131–136 (2000).
26. Lundquist, E. A., Reddien, P. W., Hartwieg, E., Horvitz, H. R. & Bargmann, C. I. Three *C. elegans* Rac proteins and several alternative Rac regulators control axon guidance, cell migration and apoptotic cell phagocytosis. *Development* **128,** 4475–4488 (2001).
27. Chou, T. B., Noll, E. & Perrimon, N. Autosomal P[ovoD1] dominant female-sterile insertions in *Drosophila* and their use in generating germ-line chimeras. *Development* **119,** 1359–1369 (1993).
28. Rajagopalan, S., Vivancos, V., Nicolas, E. & Dickson, B. J. Selecting a longitudinal pathway: Robo receptors specify the lateral position of axons in the *Drosophila* CNS. *Cell* **103,** 1033–1045 (2000).
29. Winter, C. G. *et al.* *Drosophila* Rho-associated kinase (Drok) links Frizzled-mediated planar cell polarity signaling to the actin cytoskeleton. *Cell* **105,** 81–91 (2001).
30. Chang, H. Y. & Ready, D. F. Rescue of photoreceptor degeneration in rhodopsin-null *Drosophila* mutants by activated Rac1. *Science* **290,** 1978–1980 (2000).

Acknowledgements

We thank H. Halbritter for scanning electron microscopy; P. Rørth for generating and providing the EP0855 line; T. Newsome for the initial characterization of *trio* mutant embryos; and J. Knoblich, K. Nasmyth and members of the Dickson laboratory for comments on the manuscript. This research was supported by funding from Boehringer Ingelheim GmbH (B.J.D.), and grants from the National Institutes of Health (L.L.) and the Human Frontiers of Science Program (B.J.D. and L.L.).

Competing interests statement

The authors declare that they have no competing financial interests.

Correspondence and requests for materials should be addressed to B.J.D. (e-mail: dickson@nt.imp.univie.ac.at).

Rac GTPases control axon growth, guidance and branching

Julian Ng*, Timothy Nardine*§, Matthew Harms*§, Julia Tzu*, Ann Goldstein*†, Yan Sun‡, Georg Dietzl‡, Barry J. Dickson‡ & Liqun Luo*†

* *Department of Biological Sciences, and † Neurosciences Program, Stanford University, Stanford, California 94305, USA*
‡ *Research Institute of Molecular Pathology, Dr. Bohr-Gasse 7, A-1030 Vienna, Austria*
§ *These authors contributed equally to this work*

Growth, guidance and branching of axons are all essential processes for the precise wiring of the nervous system. Rho family GTPases transduce extracellular signals to regulate the actin cytoskeleton[1]. In particular, Rac has been implicated in axon growth and guidance[2–8]. Here we analyse the loss-of-function phenotypes of three Rac GTPases in *Drosophila* mushroom body neurons. We show that progressive loss of combined Rac1, Rac2 and Mtl activity leads first to defects in axon branching, then guidance, and finally growth. Expression of a Rac1 effector domain mutant that does not bind Pak rescues growth, partially rescues guidance, but does not rescue branching defects of *Rac* mutant neurons. Mosaic analysis reveals both cell autonomous and non-autonomous functions for Rac GTPases, the latter manifesting itself as a strong community effect in axon guidance and branching. These results demonstrate the central role of Rac GTPases in multiple aspects of axon development *in vivo*, and suggest that axon growth, guidance and branching could be controlled by differential activation of Rac signalling pathways.

The *Drosophila* genome has two *Rac* genes that share 92% amino acid sequence identity and have overlapping expression patterns[2,9,10]. A highly related *Mig-2-like* (*Mtl*) gene, the orthologue of *Caenorhabditis elegans mig-2* (ref. 4), is present on the same chromosome[11,12]. To isolate loss-of-function mutants of *Rac1* and *Rac2*, we generated small deficiencies by means of imprecise excision of nearby P-elements (Fig. 1a, b). The $Rac2^{\Delta}$ excision disrupted only the *Rac2* open reading frame (ORF) (Fig. 1a), and hence is a *Rac2*-specific null mutation, but is homozygous viable. The *Df(3)Rac1* excision disrupted the *Rac1* ORF and two adjacent genes (Fig. 1b). *Rac1* point mutations were then recovered from

an ethylmethane sulphonate (EMS) screen for mutations that were lethal over *Df(3)Rac1* in a $Rac2^{\Delta}$ homozygous background, but viable in a $Rac2^{\Delta}$/+ background. Sequence analysis and transgenic rescue established that these mutants are recessive, loss-of-function *Rac1* alleles (see Methods).

Three *Rac1* missense mutations were recovered, each altering an amino acid conserved within Rho GTPases (Fig. 1c). The strongest allele, $Rac1^{J11}$, changes glycine 60 to glutamate (Gly60Glu). Structural, biochemical and genetic criteria all indicate that this is a null allele. Structurally, Gly 60 forms a hydrogen bond with the γ-phosphate of GTP, and is invariant in all members of the GTPase superfamily[13,14]. Introduction of a glutamate is predicted to disrupt this interaction. Indeed an analogous Gly60Asp mutation in H-Ras disrupts the activity of both wild-type and constitutively active proteins[15]. Biochemically, the $Rac1^{J11}$ mutation markedly impairs binding of GTP to Rac1 *in vitro*, reducing it to less than 10% compared with wild type (Fig. 1d). Genetically, homozygous $Rac1^{J11}$ phenotypes are indistinguishable from $Rac1^{J11}$/*Df(3)Rac1* in both the mushroom bodies (Fig. 2c) and visual system[12].

We used mushroom body (MB) neurons of the *Drosophila* brain to examine the role of Rac in axon development. Adult MB neurons derive from four neuroblasts per brain hemisphere. Each neuroblast sequentially generates three classes of neurons with distinct patterns of axon projection[16,17]. Each MB neuron sends a single primary neurite that gives rise to both dendritic branches and an axon. MB axons fasciculate tightly in the anteriorly projected axon peduncle. In the anterior brain, each early born class of γ-neuron has one principal medial branch, whereas each neuron of the later-born α′/β′- or α/β-classes has bifurcated axons with one dorsal (α′ or α) and one medial (β′ or β) projection[16] (Figs 2a and 3a–e). These axonal lobes can be distinguished using the fasciclin II (FasII) marker, which stains α/β-axons strongly, γ-axons weakly, but does not stain α′/β′-axons, cell bodies or dendrites of MB neurons (Fig. 3b–e).

We used three sets of experiments to analyse Rac function in MB axon development. First, by examining viable adults, we found gross axon defects in animals in which the whole brain was isogenic for particular *Rac* mutant combinations. In the second and the third sets, we used the MARCM system[18] to generate neuroblast and single-cell homozygous mutant clones that are positively labelled by MB Gal4-OK107 driven marker expression (Fig. 2b). These mosaic brains are unlikely to contain unlabelled clones outside the MB lineage, as clones were induced in newly hatched larvae, when proliferation is largely confined to the MB neuroblasts (see Methods). We found progressive defects in MB axon branching, guidance and growth as wild-type copies of *Rac1*, *Rac2* and *Mtl* (ref. 12) (referred to hereafter as Rac GTPases) were removed (Fig. 3a). Although all three Rac GTPases contribute to the fidelity of MB axon development, there is a differential dependence, with loss of *Rac1* having the largest effect and loss of *Rac2* the smallest effect (Fig. 2c, d; see also ref. 12).

Axon branching is most sensitive to loss of Rac GTPase activity. Defective branching included the generation of α- but not β-axonal branches and vice versa (Fig. 3a). This was revealed either by FasII immunostaining or expression of a murine (m)CD8–green fluorescent protein (GFP) fusion protein in the whole MB (data not shown) or in neuroblast clones (Fig. 3f–i). $Rac1^{J11}$ heterozygotes exhibited significant branching defects (Fig. 2c). The percentage of branching defects increased as additional wild-type copies of *Rac* genes were removed (Fig. 2c, d). The absence of a specific axonal lobe might be caused either by a failure of individual axons to bifurcate, or by misguidance of the bifurcated branches. To distinguish between these possibilities, we generated single-cell clones in the later-born α/β-neurons. In all cases where FasII staining revealed a branching defect in the MB as a whole ($n = 20$), only a single unbranched α- or β-axon was detected for every α/β-neuron labelled (Fig. 3h, i). These axons extended normally and followed appropriate trajectories in the remaining lobe. These observations indicate that the lack of one particular axonal lobe, as observed in isogenic (Fig. 2c) or largely isogenic mutant brains (Fig. 3h, i) or neuroblast clones (Fig. 2d, 3f), is caused by a failure in axon branching.

Axon guidance displays an intermediate sensitivity to loss of Rac GTPases. Whereas $Rac1^{J11}$ heterozygotes exhibited mainly branching defects, in $Rac1^{J11}$ homozygotes most MB axons were misguided (Fig. 2c). In mosaic animals, 21% of neuroblast clones homozygous for $Rac1^{J11}$ exhibited defective guidance (Fig. 2d). This percentage increased to 55% if the neuroblast clone was additionally homozygous for $Rac2^{\Delta}$, and to 73% if the whole brain was also heterozygous for Mtl^{Δ}(Fig. 2d). The predominant guidance defects were caused by accumulation of most or all axons in a ball-like structure at the beginning of the axon peduncle that was intensely stained for FasII (Fig. 3j, k). By labelling single mutant γ-neurons, we found that individual axons tended to wind around the FasII-positive axon 'balls', similar to those seen in the neuroblast clones (Fig. 3l, m). Therefore, these axon balls, whether they are observed in isogenic

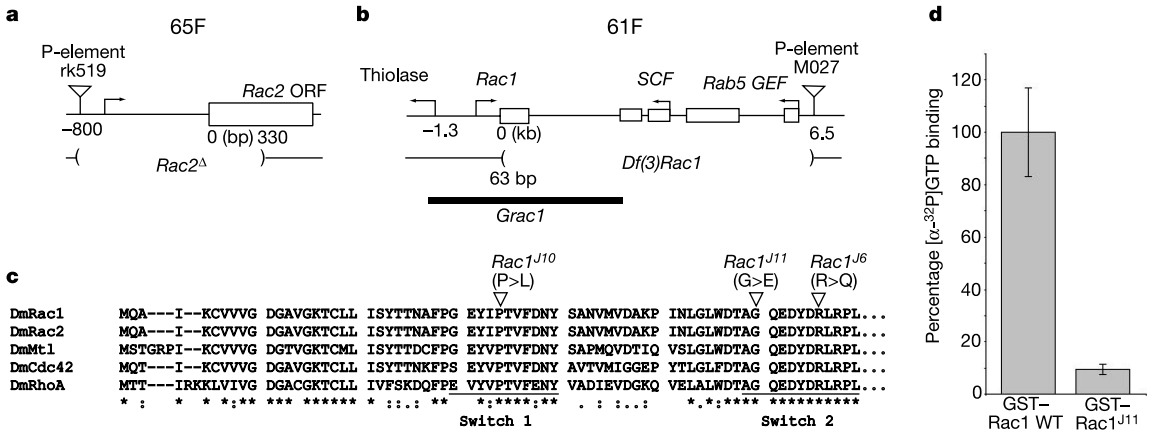

Figure 1 Loss-of-function mutants in *Drosophila Rac1* and *Rac2*. **a**, **b**, Genomic organizations of the *Rac2* (**a**) and *Rac1* (**b**) loci. P-element positions, extent of the deletions and the genomic *Rac1* rescue construct (*Grac1*) are shown. Boxes, ORFs; arrows, transcription initiation sites and directions. 65F and 61F indicate cytogenetic location. **c**, N-terminal residues for five *Drosophila melanogaster* (DM) Rho-family small GTPases are aligned, with two 'switch' regions[13] underlined. Asterisks, identical residues; colons, conserved residues; full stop, residues conserved in two or three genes. Positions and amino-acid changes of three *Rac1* missense mutants are indicated. **d**, Quantification of GTP-binding activities of wild-type and Rac1G60E ($Rac1^{J11}$) proteins. Average wild-type activity is set at 100%. Error bars indicate standard error ($n = 3$).

mutant brains, neuroblast clones, or single neuron clones, are caused by misguidance of MB axons.

Axon growth is least sensitive to loss of Rac GTPases. Defects in axon growth were found mainly in MB neurons homozygous for $Rac1^{J11}$ $Rac2^{\Delta}$ Mtl^{Δ} (Fig. 2d). Ball-like axon accumulations were only rarely observed in this genotype. Instead, these axons terminated prematurely or failed to enter FasII-positive regions altogether (Fig. 3n–o). Most of the remaining axons exhibited severe guidance defects, extending their axons in a non-stereotypical fashion. To confirm our interpretation of a growth defect, we examined single-cell clones homozygous for $Rac1^{J11}$ $Rac2^{\Delta}$ Mtl^{Δ} in brain hemispheres in which most of the FasII-positive γ-axons (representing non-clonal tissue) were correctly patterned as in wild type. We found that 55% of homozygous $Rac1^{J11}$ $Rac2^{\Delta}$ Mtl^{Δ} single-cell clones exhibited axon-stalling defects, mostly at the peduncle (Figs 3p, q and 4b), as compared with less than 5% in $Rac1^{J11}$ $Rac2^{\Delta}$ single-cell clones ($n > 100$). These data indicate that Rac1, Rac2 and Mtl collaborate to control axon growth in a cell-autonomous manner.

The dendritic region of MB neuroblast clones homozygous for $Rac1^{J11}$ $Rac2^{\Delta}$ Mtl^{Δ} still possessed mCD8–GFP-positive neurites, which were presumably contributed by the initial neurite outgrowth from the cell body and elaboration of MB dendrites (Fig. 3m–o). Quantitative analysis of single-cell $Rac1^{J11}$ $Rac2^{\Delta}$ Mtl^{Δ} clones revealed significant reduction in both total dendritic length (wild type, 66.3 ± 5.8 μm; mutant, 49.6 ± 4.7 μm, $n = 16$ and 13, respectively) and number of dendritic segments per neuron (wild type, 18.1 ± 1.8; mutant, 11.4 ± 1.6, $n = 16$ and 13, respectively), indicating that Rac GTPases are also required for dendritic growth and branching.

The differential sensitivity of axon growth, guidance and branching to loss of Rac function could in principle reflect the fact that axons must grow in order to be assayed for guidance and branching defects, and may need correct guidance to reach appropriate branching points. However, such a simple hierarchical model cannot explain our data. If Rac were equally required for growth, guidance and branching, and these processes were simply epistatic to one another as proposed by this heirarchical model, then growth defects should always be more frequent than guidance defects, which in turn should always be more frequent than branching defects. For example, if growth, guidance and branching were equally reduced by 20%, then in a population of 100 axons, 20 would show a growth defect, 16 would show a guidance defect (20% of the 80 axons that grow), and 13 would show a branching defect (20% of the 64 axons that grow and navigate correctly). However, this is not what we observed; instead, we saw a shift from branching to guidance to growth defects as the combined level of wild type Rac is progressively reduced (Fig. 2c–d). That axon branching can be selectively perturbed is best exemplified in genotypes involving a hypomorphic allele $Rac1^{J10}$ (Fig. 2c, d). Furthermore, axon branching defects could be disrupted without any growth or guidance defects (Fig. 3f–i), whereas guidance could be disrupted without obvious growth defects (Fig. 3l, m). These data strongly suggest that axon growth, guidance and branching are separable events requiring increasing amounts of combined Rac GTPase activity *in vivo*.

One model that could account for these observations is that growth, guidance and branching use different Rac effector pathways. To test this idea, we made use of Rac effector domain mutants. The Rac Phe37Ala mutation (RacF37A) abolishes the ability of activated Rac to induce lamellipodia formation without affecting the Pak/JNK pathway. However, the Rac Tyr40Cys mutation (RacY40C) blocks Rac binding to effectors containing the 'CRIB' motif, including Pak[19–22], but does not affect lamellipodia formation[19,20] (Fig. 4a). Overexpression of analogous Rac1F37A and Rac1Y40C mutants, or wild-type Rac1, did not disrupt MB axon patterning in a wild-type background (Fig. 4c). We could therefore use the MARCM system to express these effector mutants specifically in Rac mutant clones to determine which effector pathways are required for MB axon growth, guidance and branching.

MB axon growth defects in single-cell $Rac1^{J11}$ $Rac2^{\Delta}$ Mtl^{Δ} clones were largely rescued by transgenic expression of wild-type Rac1 or Rac1Y40C, but not Rac1F37A (Fig. 4b), indicating that direct binding of CRIB effector proteins are not required for Rac function in axon growth. To assess the effector pathways involved in guidance and branching, we expressed these same transgenes in $Rac1^{J11}$ $Rac2^{\Delta}$ neuroblast clones. In this background, 81% of axons show mutant phenotypes, predominantly guidance (55%) and branching (24%) defects. Expression of wild-type Rac1 markedly rescued these defects, reducing the fraction of abnormal axon phenotypes to 53% (Fig. 4c). The remaining branching and guidance defects were probably caused by influences of nearby non-clonal MB neurons (see below) heterozygous for $Rac1^{J11}$ $Rac2^{\Delta}$, which exhibited a similar degree of branching and guidance defects (Fig. 2c). Neither Rac1Y40C nor Rac1F37A expression reduced the percentage of total

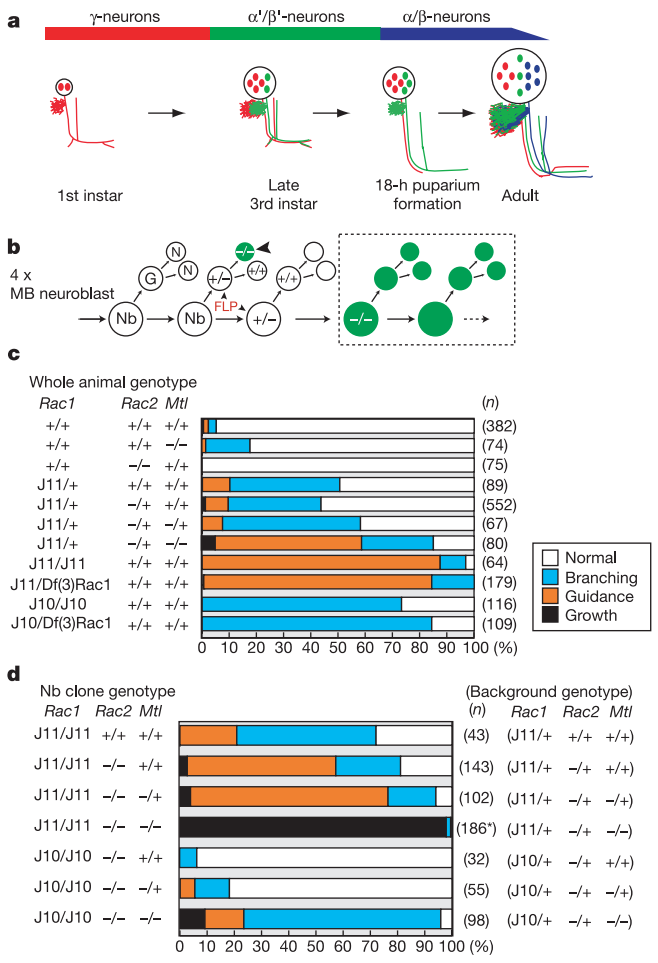

Figure 2 Quantitative phenotypic analysis of Rac GTPases in MB axon branching, guidance and growth. **a**, Schematic summary of MB development[16]. **b**, Schematic of MB neuroblast division pattern, illustrating FLP-induced mitotic recombination and the generation of homozygous mutant (–/–) neuroblast clones (boxed) or single-cell MB clones (arrowhead) that are uniquely marked (green) via the MARCM system[18]. Nb, neuroblast; G, ganglion mother cell; N, post-mitotic neuron. **c**, Percentages of MB axon branching, guidance and growth defects in adult viable and isogenic *Rac* mutants. **d**, Percentages of branching, guidance and growth defects in *Rac* mutant MB neuroblast clones, generated and labelled via MARCM. Most growth defects in triple mutant neuroblast clones are also associated with severe guidance errors (indicated with an asterisk). *n*, number of brain hemispheres (**c**) or neuroblast clones (**d**) examined. All chromosomes except $Rac2^{\Delta}$ and Mtl^{Δ} are in the FRT^{2A} background, which when homozygous consistently gives a small percentage of errors in MB axon development.

axonal defects (78% and 88%, respectively). However, expression of Rac1Y40C (but not Rac1F37A) resulted in a marked shift in the distribution of axonal defects, with most showing branching (45%) rather than guidance (31%) defects. Thus, compared with wild-type Rac1, expression of Rac1Y40C in a Rac mutant background was able to rescue growth, partially rescue guidance, but was unable to rescue branching defects (Fig. 4d).

These results suggest that different downstream effector pathways mediate axon growth, guidance and branching. In particular, Rac binding of CRIB-domain effectors such as Pak is not required for axon growth, but may contribute to axon guidance and branching. This is consistent with genetic analyses indicating a requirement for *Drosophila* Pak in axon guidance but not growth[11,23].

Our mosaic analysis revealed an unexpected degree of cell non-autonomous effects in axon guidance and branching caused by defective Rac activity. If every MB axon were to choose its pathway

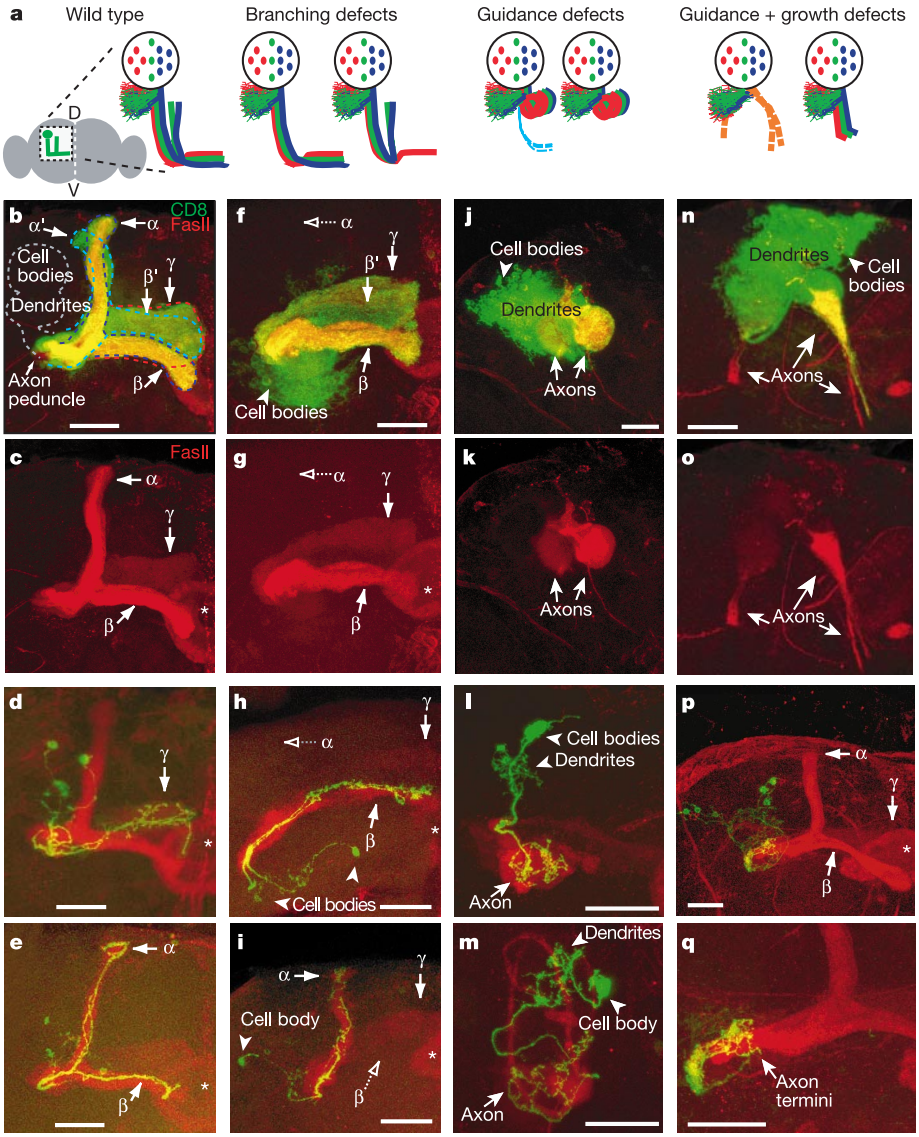

Figure 3 Images of wild-type and *Rac* mutant MB axons. **a**, Schematic summary of branching, guidance and growth defects in *Rac* mutant MB neurons. All drawings and images (**b**–**q**, Z-projections of confocal sections) are of adult MB of the left hemisphere, roughly from the boxed region in the scheme of the brain on the left. D, dorsal; V, ventral. The white dashed line indicates the midline. Green, neuroblast or single-cell MARCM clones (sometimes multiple single-cell clones) immunostained with anti-CD8 antibodies; red, FasII staining of all MB γ- and α/β-axons. **b**–**e**, Wild-type MB axons in neuroblast clones (**b**), two single-cell clones of γ-neurons (**d**) or α/β-neurons (**e**). The extent of each axonal lobe is outlined in **b** and labelled with arrows. **f**–**i**, *Rac* mutant MB neuroblast clones (**f**) and two (**h**) or one (**i**) single-cell clones of α/β-neurons exhibiting axon branching defects. Filled or open arrows point to existing or missing lobes, respectively. **j**–**m**, *Rac* mutant MB neuroblast clones (**j**) and two-cell (**l**) or single-cell (**m**) clones of γ-neurons exhibiting axon guidance defects. **n**, **o**, *Rac* mutant MB neuroblast clones exhibiting axon growth and guidance defects. **p**, **q**, Six single-cell clones exhibiting axon growth defects in a brain hemisphere where global MB axon patterning is relatively normal, as revealed by FasII staining. **q**, Higher magnification of **p**. Arrow points to axon termini at the peduncle before the branching point. **c**, **g**, **k**, **o** are the same as **b**, **f**, **j** and **n**, respectively, showing only FasII staining. Asterisk indicates the ellipsoid body, a central brain structure also stained with FasII. Scale bars, 20 μm. Genotypes within the clones: **b**–**e**, FRT^{2A}; **f**–**l**, $Rac1^{J11}$ $Rac2^{\Delta}$ FRT^{2A}; **m**–**q**, $Rac1^{J11}$ $Rac2^{\Delta}$ FRT^{2A} Mtl^{Δ}. Genotypes outside the clones: **b**–**e**, FRT^{2A}; **f**–**l**, $Rac1^{J11}/+$, $Rac2^{\Delta}/+$, FRT^{2A}; **m**–**q**, $Rac1^{J11}/+$, $Rac2^{\Delta}/+$, FRT^{2A}, Mtl^{Δ}. Cell body positions vary as labelled clones can be derived from any of the four MB neuroblasts. In some cases, MB cell bodies, dendrites and axonal peduncles overlap with the axonal lobes in the *x*–*y* plane, and were removed from the projection, or replaced with a cartoon (**a**). We did not observe obvious reduction of the number of MB neurons in $Rac1^{J11}$ $Rac2^{\Delta}$ neuroblast clones, but observed a slight reduction in $Rac1^{J11}$ $Rac2^{\Delta}$ Mtl^{Δ} neuroblast clones.

independently, then in a brain hemisphere containing one homozygous *Rac1*^{J11} *Rac2*$^{\Delta}$ neuroblast and three heterozygous neuroblasts, one would expect to observe a mixture of wild-type and mutant trajectories. Remarkably, all FasII-positive axons in the same hemisphere as the mutant neuroblast clone invariably exhibited the same guidance defect (compare Fig. 3k with j). This cannot be explained simply by the guidance defect caused by *Rac1*^{J11} *Rac2*$^{\Delta}$ heterozygous neurons, as only 8% of such hemispheres exhibited this defect (Fig. 2c). Such a cell non-autonomous effect was also observed in axon branching. If every branching-defective α/β-neuron were to make an independent decision to form either a single dorsal or medial branch, then in neuroblast clones where hundreds of axons are examined together, one would expect to see a thinning of both axonal lobes rather than the absence of a single lobe. Instead, in *Rac1*^{J11} *Rac2*$^{\Delta}$ neuroblast clones that exhibited branching defects, all MB axons in the neuroblast clone projected either dorsally (one-third) or medially (two-thirds). Most non-clonal axons (as revealed by FasII staining) would always make the same choice as the mutant clone (Fig. 3f, g). Whereas homozygous mutant axons could induce their heterozygous neighbours to make the same errors, it is possible that heterozygous axons could reduce the error rate of nearby homozygous mutant axons. This could be one explanation for why the phenotypes of homozygous mutant animals are of higher penetrance than those of homozygous mutant neuroblast clones (compare Fig. 2c with d).

These observations suggest a marked community effect in MB axon guidance and branching: axons of mixed genotypes make their choices together. In any given animal, the collective choice of a normal versus mutant projection is likely to be influenced by the severity of the genotype, and the relative number of homozygous versus heterozygous axons. Such collective decision making is probably a result of tight fasciculation among MB axons, which is not disrupted in *Rac* mutants. It will be interesting to test whether this community effect reflects a general feature of axon development in a complex central nervous system environment.

Our analysis of Rac GTPases in MB axon development suggests a mechanistic link between axon growth, guidance and branching. Although there is evidence that axon growth and guidance have different cytoskeletal requirements[24–26], their connections are not well understood[6]. Little is known about intracellular signalling mechanisms that regulate axon branching[27,28]. Here we show that axon growth, guidance and branching require increasing amounts of combined Rac GTPase activity *in vivo* (Figs 2c, d and 4b, d). In the accompanying paper, we report similar differential requirements for Rac activity in embryonic axon growth and guidance[12]. The requirement of Rac GTPases for axon outgrowth and guidance in *C. elegans* has also been reported recently[8]. We propose (Fig. 4d) that axon branching, guidance and growth specified by extracellular cues require different amount of Rac GTPase activation in the growth cone, which in turn engage different downstream pathways to specify distinct cytoskeletal changes. □

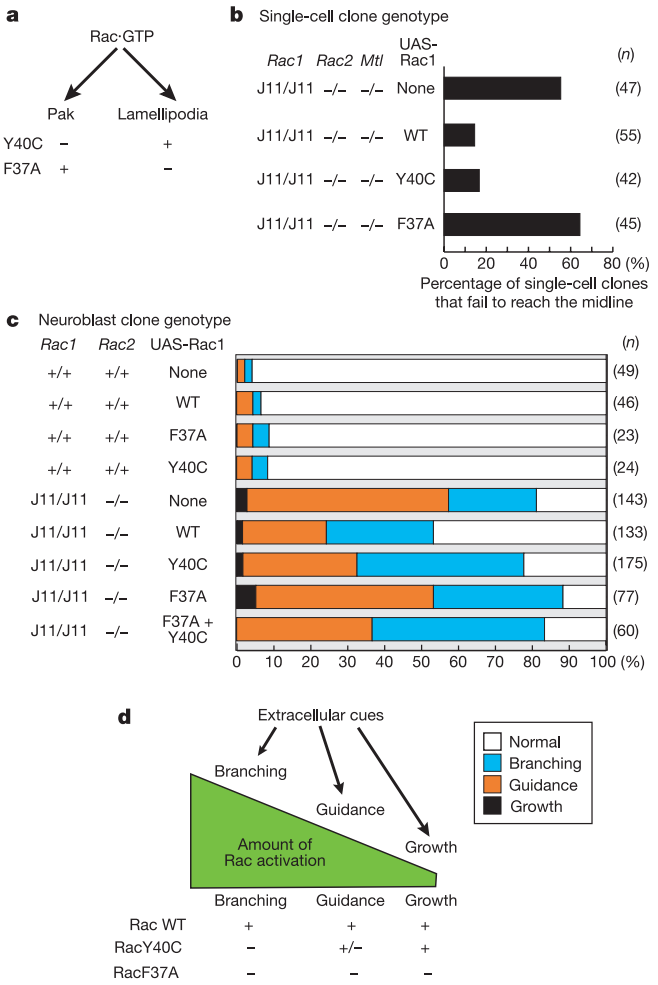

Figure 4 Effector domain mutant analysis. **a**, Specificity of Rac effector domain mutants in activating Pak kinase or inducing lamellipodial formation. **b**, Quantification of axon growth defects of *Rac1*^{J11} *Rac2*$^{\Delta}$ *Mt*$^{\Delta}$ single-cell clones in the absence or presence of *Rac1* transgenes overexpressing wild-type (WT) or effector domain mutants. *n*, number of single-cell γ-neuron clones examined. **c**, Percentage of branching, guidance and growth defects in *Rac1*^{J11} *Rac2*$^{\Delta}$ neuroblast clones in the absence or presence of *Rac1* transgenes overexpressing wild-type or effector domain mutants. *n*, number of neuroblast clones examined. Also shown are the effects of expressing these transgenes in control flies (*FRT*^{2A}). **d**, Schematic summary and a working hypothesis. See text for details.

Methods

Genetics and molecular biology

P-elements near *Rac1* and *Rac2* were obtained from the Berkeley Drosophila Genome Project. Insertion sites were determined by inverse polymerase chain reaction (PCR). We generated *Rac2* null alleles via imprecise excision of P-element rk519. Imprecise excision of P-element M027 yielded flies carrying a 6.4-kilobase (kb) deletion (which we named *Df(3)Rac1*) from the insertion site to codon 21 of *Rac1*, abolishing *Rac1* function but also removing two other genes (Fig. 1b). *Rac1*-specific mutations were isolated by screening through 8,500 chromosomes mutagenized with EMS for those that failed to complement *Df(3)Rac1* in a *Rac2*$^{\Delta}$ homozygous background. In a *Rac2*$^{\Delta}$ homozygous background, these lethal mutations could be rescued to full viability and fertility with a transgene carrying a genomic fragment of the *Rac1* gene (*Grac1*, Fig. 1b). To generate *Grac1*, a 3.6-kb genomic fragment containing the entire transcription unit and flanking DNA of *Rac1* was subcloned from a P1 clone (DS06962) into the transformation vector pW8 to obtain germline transformants. To determine the molecular identity of *Rac1* mutations, genomic DNA encompassing the *Rac1* ORF was amplified from mutants by PCR, and sequenced. Effector domain mutants were constructed via site-directed mutagenesis, verified by sequencing, subcloned into a vector containing two copies of an amino-terminal Myc tag, and finally into pUAST for germline transformation.

GTP-binding assay

Wild-type *Rac1* and *Rac1*^{J11} were amplified by PCR and subcloned into pGEX 4T-1 to express as glutathione *S*-transferase (GST) fusion proteins in strain BL21. We performed GTP binding assays according to methods described previously[29]. [α-^{32}P]GTP bound to GST beads was used as the baseline of GTP binding. GTP binding of Rac1 was dependent on Mg^{2+} (data not shown).

MARCM analysis

The MARCM system uses FLP recombinase to induce site-specific mitotic recombination. (FLP, flippase; FRT, FLP recognition target.) Neuroblast and single-cell clones were generated using *hs-FLP* and the 3L *FRT*^{2A}, and visualized by mCD8–GFP expression driven by Gal4-OK107, which labels all MB neurons, as described previously[16]. All MARCM clones except those shown in Fig. 3h, i were generated by heat-shock-induced FLP expression in newly hatched larvae, when neuroblast proliferation and clone generation is largely limited to MB neuroblasts[16,18,30]. Neuroblast clones generated in this fashion comprise approximately one-quarter of all MB neurons in a given brain hemisphere with all three classes of MB neurons. Single-cell clones are exclusively γ-neurons. These are particularly useful for phenotypic analysis in adults, as the larval-specific axon branches are pruned and adult-specific branches are not generated until 4–5 days after clone generation[16], thus minimizing the continuing presence of Rac protein from the time of clone generation to the time of axon re-extension. To generate single-cell

α/β-neuron clones, for studying branching, heat shock was applied at the pupal stage, when MB neuroblasts are again the predominant dividing neuroblast[18,30]. We also used the MARCM system for Gal4-induced UAS-transgene expression specifically in MB clones for rescue experiments (Fig. 4b, c). Myc-tagged Rac1 or effector domain mutants (Myc-Rac1Y40C or Myc-Rac1F37A) were expressed at similar levels, as judged by Myc-staining.

Immunohistochemistry and image analyses

Isogenic or mosaic mutant brains were dissected within 3–7 days after eclosion, fixed, immunostained for mCD8 and FasII, and imaged as described previously[16]. For quantifying MB dendrites, confocal images taken at 0.5 μm were traced using the Neurolucida software. The total numbers of branch segments and branch length were quantified using Neuroexplorer (mean ± standard errors are presented).

Received 1 August 2001; accepted 31 January 2002.

1. Hall, A. Rho GTPases and the actin cytoskeleton. *Science* **279,** 509–514 (1998).
2. Luo, L., Liao, Y. J., Jan, L. Y. & Jan, Y. N. Distinct morphogenetic functions of similar small GTPases: *Drosophila* Drac1 is involved in axonal outgrowth and myoblast fusion. *Genes Dev.* **8,** 1787–1802 (1994).
3. Kozma, R., Sarner, S., Ahmed, S. & Lim, L. Rho family GTPases and neuronal growth cone remodelling: relationships between increased complexity induced by Cdc42Hs, Rac1, and acetylcholine and collapse induced by RhoA and lysophosphatidic acid. *Mol. Cell. Biol.* **17,** 1201–1211 (1997).
4. Zipkin, I. D., Kindt, R. M. & Kenyon, C. J. Role of a new Rho family member in cell migration and axon guidance in *C. elegans*. *Cell* **90,** 883–894 (1997).
5. Kaufmann, N., Wills, Z. P. & Van Vactor, D. *Drosophila* Rac1 controls motor axon guidance. *Development* **125,** 453–461 (1998).
6. Luo, L. Rho GTPases in neuronal morphogenesis. *Nature Rev. Neurosci.* **1,** 173–180 (2000).
7. Dickson, B. J. Rho GTPases in growth cone guidance. *Curr. Opin. Neurobiol.* **11,** 103–110 (2001).
8. Lundquist, E. A., Reddien, P. W., Hartwieg, E., Horvitz, H. R. & Bargmann, C. I. Three *C. elegans* Rac proteins and several alternative Rac regulators control axon guidance, cell migration and apoptotic cell phagocytosis. *Development* **128,** 4475–4488 (2001).
9. Hariharan, I. K. *et al.* Characterization of rho GTPase family homologues in *Drosophila melanogaster*: overexpressing Rho1 in retinal cells causes a late developmental defect. *EMBO J.* **14,** 292–302 (1995).
10. Harden, N., Loh, H. Y., Chia, W. & Lim, L. A dominant inhibitory version of the small GTP-binding protein Rac disrupts cytoskeletal structures and inhibits developmental cell shape changes in *Drosophila*. *Development* **121,** 903–914 (1995).
11. Newsome, T. *et al.* Trio combines with dock to regulate Pak activity during photoreceptor axon pathfinding in *Drosophila*. *Cell* **101,** 283–294 (2000).
12. Hakeda-Suzuki, S. *et al.* Rac function and regulation during *Drosophila* development. *Nature* **416,** 438–442 (2002).
13. Bourne, H. R., Sanders, D. A. & McCormick, F. The GTPase superfamily: conserved structure and molecular mechanism. *Nature* **349,** 117–127 (1991).
14. Worthylate, D. K., Rossman, K. L. & Sondek, J. Crystal structure of Rac1 in complex with the guanine nucleotide exchange region of Tiam1. *Nature* **408,** 682–688 (2000).
15. Mosteller, R. D., Han, J. & Broek, D. Identification of residues of the H-ras protein critical for functional interaction with guanine nucleotide exchange factors. *Mol. Cell Biol.* **14,** 1104–1112 (1994).
16. Lee, T., Lee, A. & Luo, L. Development of the *Drosophila* mushroom bodies: sequential generation of three distinct types of neurons from a neuroblast. *Development* **126,** 4065–4076 (1999).
17. Ito, K., Awano, W., Suzuki, K., Hiromi, Y. & Yamamoto, D. The *Drosophila* mushroom body is a quadruple structure of clonal units each of which contains a virtually identical set of neurons and glial cells. *Development* **124,** 761–771 (1997).
18. Lee, T. & Luo, L. Mosaic analysis with a repressible cell marker for studies of gene function in neuronal morphogenesis. *Neuron* **22,** 451–461 (1999).
19. Lamarche, N. *et al.* Rac and Cdc42 induce actin polymerization and G1 cell cycle progression independently of p65PAK and the JNK/SAPK MAP kinase cascade. *Cell* **87,** 519–529 (1996).
20. Joneson, T., McDonough, M., Bar-Sagi, D. & Van Aelst, L. RAC regulation of actin polymerization and proliferation by a pathway distinct from Jun kinase. *Science* **274,** 1374–1376 (1996).
21. Morreale, A. *et al.* Structure of Cdc42 bound to the GTPase binding domain of PAK. *Nature Struct. Biol.* **7,** 384–388 (2000).
22. Owen, D., Mott, H. R., Laue, E. D. & Lowe, P. N. Residues in Cdc42 that specify binding to individual CRIB effector proteins. *Biochemistry* **39,** 1243–1250 (2000).
23. Hing, H., Xiao, J., Harden, N., Lim, L. & Zipursky, S. Pak functions downstream of Dock to regulate photoreceptor axon guidance in *Drosophila*. *Cell* **97,** 853–863 (1999).
24. Yamada, K. M., Spooner, B. S. & Wessells, N. K. Axon growth: roles of microfilaments and microtubules. *Proc. Natl Acad. Sci. USA* **66,** 1206–1212 (1970).
25. Marsh, L. & Letourneau, P. C. Growth of neurites without filopodial or lamellipodial activity in the presence of cytochalasin B. *J. Cell. Biol.* **99,** 2041–2047 (1984).
26. Bentley, D. & Toroian-Raymond, A. Disoriented pathfinding by pioneer neurone growth cones deprived of filopodia by cytochalasin treatment. *Nature* **323,** 712–715 (1986).
27. Scott, E. K. & Luo, L. How do dendrites take their shape? *Nature Neurosci.* **4,** 359–365 (2001).
28. Wang, K. H. *et al.* Biochemical purification of a mammalian slit protein as a positive regulator of sensory axon elongation and branching. *Cell* **96,** 771–784 (1999).
29. Knaus, U. G., Heyworth, P. G., Kinsella, B. T., Curnutte, J. T. & Bokoch, G. M. Purification and characterization of Rac2. *J. Biol. Chem.* **267,** 23575–23582 (1992).
30. Ito, K. & Hotta, Y. Proliferation pattern of postembryonic neuroblasts in the brain of *Drosophila melanogaster*. *Dev. Biol.* **149,** 134–148 (1992).

Acknowledgements

We thank the Berkeley Drosophila Genome Project for providing the P-elements, C. Goodman for the FasII antibody, and members of the Luo laboratory and M. Tessier-Lavigne for critical reading of the manuscript. J. N. was partly supported by a postdoctoral fellowship from the American Cancer Society California Division. This research was supported by grants from the National Institutes of Health to L.L., and from the Human Frontiers Science Program to L.L. and B.J.D.

Competing interests statement

The authors declare that they have no competing financial interests.

Correspondence and requests for materials should be addressed to L.L. (e-mail: lluo@stanford.edu).

Calmodulin interacts with MLO protein to regulate defence against mildew in barley

Min C. Kim*†§, Ralph Panstruga†§, Candace Elliott‡, Judith Müller†, Alessandra Devoto‡, Hae W. Yoon*, Hyeong C. Park*, Moo J. Cho* & Paul Schulze-Lefert†

** Division of Applied Life Science (BK21 program), Plant Molecular Biology & Biotechnology Research Centre, Gyeongsang National University, Chinju 660-701, Korea*

† Max-Planck-Institut für Züchtungsforschung, Department of Plant Microbe Interactions, Carl-von-Linné-Weg 10, D-50829 Köln, Germany

‡ The Sainsbury Laboratory, John Innes Centre, Colney Lane, Norwich NR4 7UH, UK

§ These authors contributed equally to this work

In plants, defence against specific isolates of a pathogen can be triggered by the presence of a corresponding race-specific resistance gene[1], whereas resistance of a more broad-spectrum nature can result from recessive, presumably loss-of-regulatory-function, mutations[2]. An example of the latter are *mlo* mutations in barley, which have been successful in agriculture for the control of powdery mildew fungus (*Blumeria graminis* f. sp. *hordei*; *Bgh*)[3]. MLO protein resides in the plasma membrane, has seven transmembrane domains, and is the prototype of a sequence-diversified family unique to plants[4,5], reminiscent of the seven-transmembrane receptors in fungi and animals[5]. In animals, these are known as G-protein-coupled receptors and exist in three main families, lacking sequence similarity, that are thought to be an example of molecular convergence[6]. MLO seems to function independently of heterotrimeric G proteins. We have identified a domain in MLO that mediates a Ca^{2+}-dependent interaction with calmodulin *in vitro*. Loss of calmodulin binding halves the ability of MLO to negatively regulate defence against powdery mildew *in vivo*. We propose a sensor role for MLO in the modulation of defence reactions.

We adopted a genetic approach to test for the possible involvement of heterotrimeric G proteins in MLO-dependent defence modulation. Unlike metazoans, plants generally have only one gene coding for a canonical heterotrimeric G-protein α-subunit (ref. 7, and J. Glazebrook, personal communication). Southern blot analysis revealed that barley also contains a single-copy gene for Gα (*HvGα*; data not shown). We isolated a full-length *HvGα* complementary DNA and generated three nominally constitutive active variants, HvGα G48V, HvGα R191C and HvGα Q223L, for testing in barley-leaf epidermal cells, using a system for delivering the DNA constructs on microprojectiles[8]. Each of the substitutions involves a residue within the GTP-binding domain that is invariant among Gα proteins (Supplementary Information 1), and has been shown to inhibit the intrinsic GTPase activity of animal, fungal and plant Gα